Catal Lett (2008) 120:215–220
DOI 10.1007/s10562-007-9272-9

Preparation, Characterization and Catalytic Activity for CO Oxidation of SiO_2 Hollow Spheres Supporting CuO Catalysts

Chunyan Song · Chunling Wang · Haiyang Zhu · Xingcai Wu · Lin Dong · Yi Chen

Received: 1 August 2007 / Accepted: 29 August 2007 / Published online: 21 September 2007

Abstract Silica hollow spheres were synthesized by sol–gel process using carbon microspheres as templates, and used as supports for CuO/SiO_2 catalysts. The samples were characterized by TEM, nitrogen adsorption–desorption, XRD and TPR, and furthermore, the catalytic performance for CO oxidation was approached. The results indicated that the catalytic activity of CuO supported on SiO_2 hollow spheres exhibited much higher as compared to that supported on commercial SiO_2. Enhancement of the catalytic activity may be attributed to the fact that the unique hollow spherical texture should facilitate the formation of main active species and gas diffusion in catalysts.

Keywords Hollow spheres · CuO/SiO_2 · CO oxidation · Catalytic activity

1 Introduction

Hollow spheres have increasingly attracted interest due to their unique properties and potential applications in chemistry, biotechnology, and materials science [1–3]. Inorganic materials with hollow spherical structure have exhibited excellent properties in many aspects such as magnetic, optical [4–6] and electric properties [7, 8]. However, little attentions have been paid to the research on catalytic properties of hollow spheres in the past years. Recently, the hollow spheres as catalysts have been applied to several liquid phase reactions [9–11]. For example, the PdCo bimetallic hollow spheres were successfully applied to catalysis of the Sonogashira Reaction [12].

In recent years, the CO catalytic oxidation has become an important research topic because of its various applications in pollution control devices for vehicle exhaust, CO gas sensors, and catalytic combustion, and so on [13–15]. Copper-contained catalysts show a potential activity for the CO oxidation and have been extensively investigated during the past decades [16–18]. It is well known that SiO_2 is a good catalyst support and the performance of catalysts has a close relationship with the properties of supports [19–23]. Therefore, silica with hollow spherical structure was selected as supports of copper oxide (CuO) in present work, in order to study the influence of morphology of supports on catalytic activity.

Herein we used carbon spheres as templates [24] to fabricate silica hollow spheres by a succinct sol–gel path and researched the catalytic performance for $CO + O_2$ reaction. The results indicated that catalytic activity of CuO supported on SiO_2 hollow spheres exhibited much higher as compared to that supported on commercial SiO_2. The possible reason of this phenomenon was also discussed.

2 Experimental

2.1 Preparation of CuO/SiO_2 Hollow Spheres Catalysts

The templates of carbon microspheres were synthesized through the polycondensation reaction of glucose under

C. Song · C. Wang · H. Zhu · X. Wu (✉) · L. Dong (✉) · Y. Chen
Key Laboratory of Mesoscopic Chemistry of MOE, School of Chemistry and Chemical Engineering, Nanjing University, Nanjing 210093, P.R. China
e-mail: wuxingca@nju.edu.cn

L. Dong
e-mail: donglin@nju.edu.cn

hydrothermal conditions. The surface of the spheres is hydrophilic and has many hydroxyl groups [25]. Figure 1 shows the overall procedure used to synthesize the hollow spherical catalysts. All the reagents used in this investigation are analytical grade and without further purification. The carbon microspheres templates were dispersed in ethanol, and then 25 wt.% aqueous ammonia was added to adjust the pH value of the suspension to 9. The desired amount of TEOS/ethanol mixture was dropped into the dispersion so that a sol–gel process was carried out, stirring for 24 h. A core/shell composite nanostructure with SiO_2 coating the carbon spheres was obtained after centrifugation and drying. Then, the nanostructure was heated at the rate of 3 °C/min and calcined at 500 °C for 4 h in air to produce SiO_2 hollow spheres. The SiO_2 hollow spheres were impregnated in an aqueous solution containing the requisite amount of copper nitrate hexahydrate, then dried at 100 °C, and followed by calcinations at 500 °C in air for 7 h. For comparison, CuO-supported commercial SiO_2 catalysts were prepared according to the same process. The commercial SiO_2 is a highly porous silica aerogel, which was calcined at 500 °C for 4 h in air before used.

For the sake of simplicity, the hollow spheres catalysts were signed as H-xCuSi (x = 2, 10, 20), which corresponded to 2 g CuO/100 g SiO_2, 10 g CuO/100 g SiO_2, and 20 g CuO/100 g SiO_2, respectively. Similarly, the commercial SiO_2 with different CuO loading amounts catalysts were signed as C-xCuSi.

2.2 Characterization

The size and morphology of the products were observed by using a Hitachi Model H-800 transmission electron microscope (TEM), with a tungsten filament at an accelerating voltage of 200 kV. Nitrogen adsorption–desorption isotherms were obtained at 77 K on a Micromeritics ASAP 2020 apparatus, and the pore size distribution was calculated from the nitrogen desorption isotherm by the Barrett–Joyner–Halenda (BJH) method. The phase analysis of the products was examined by X-ray diffraction (XRD) using a Philips X'pert Pro diffractometer with Ni-filtered CuKa radiation (0.15418 nm). The X-ray tube was operated at 40 kV and 40 mA.

Temperature-programmed reduction (TPR) was carried out in a quartz U-tube reactor, and a 100 mg sample was used for each measurement. Prior to the reduction, the sample was pretreated in a N_2 stream at 100 °C for 1 h and then cooled to room temperature. After that, a H_2–Ar mixture (7% H_2 by volume) was switched on, and the temperature was increased linearly at a rate of 10 °C/min. A thermal conductivity cell detected the consumption of H_2 in the reactant stream.

The activities of the catalysts for CO + O_2 reaction were carried out under steady state, involving a feed stream with a fixed composition 1.6% CO, 20.8% O_2 and 77.6% N_2 by volume. A quartz tube was employed as the reactor and the requisite quantity of catalysts (25 mg for each test) were

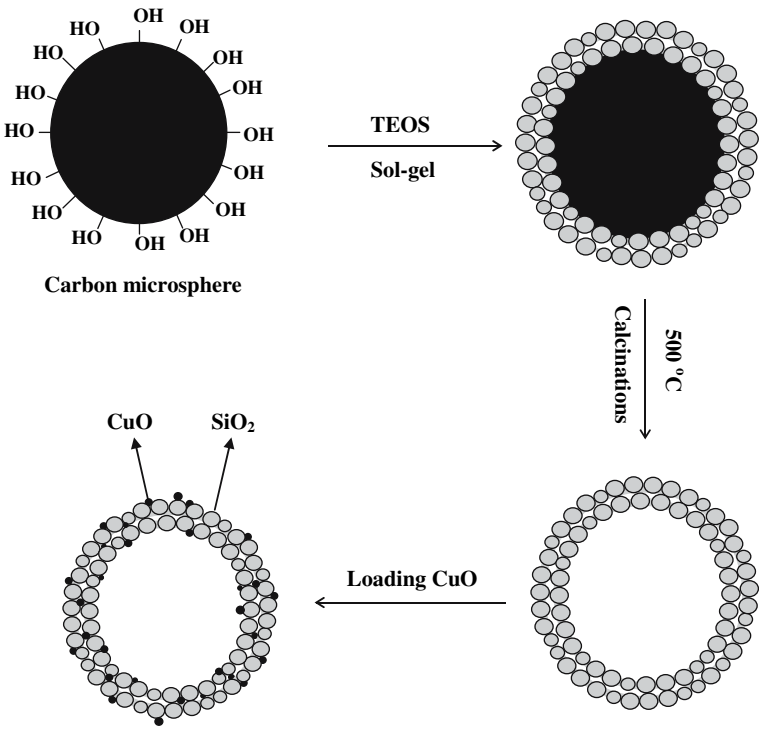

Fig. 1 Schematic representation of the formation of SiO_2 hollow spheres supporting CuO catalysts by using carbonaceous microspheres as templates

used. The catalysts were pretreated in N_2 stream at 100 °C for 1 h and then heated to reaction temperature, after that, the mixed gases were switched on. The reactions were carried out at different temperatures with the same space velocity of 30,000 mL g^{-1} h^{-1}. Two chromatogram columns and thermal conduction detection (TCDs) were used for the purpose of analyzing the production. Column A was packed with 13X molecular sieve (30–60 M) for separating O_2, N_2 and CO while column B packed with Porapak Q for monitoring CO_2.

3 Results and Discussion

As shown in Fig. 2a, the diameter of the hollow spheres is about 1 μm and the average wall thickness is about 100 nm. After impregnation and calcinations, the hollow spherical structure of catalysts could be preserved (Fig. 2 b). Figure 2c provides further insight into the structure of the shell wall, indicating that the walls of the hollow spheres are constructed by numerous small silica particles connecting each other and with an average diameter of about 80 nm. Furthermore, it should be noted that there are gaps among SiO_2 particles. As presented in Fig. 2d, commercial SiO_2 are the irregular assembly of numerous small silica particles, and the size of silica particles is about 20 nm.

Figure 3 presents the nitrogen adsorption–desorption isotherms and the corresponding pore size distribution plots (insets) for commercial SiO_2 and SiO_2 hollow spheres. The isotherms of type IV with H3 type hysteresis loops are obtained. This result verifies that both the supports have porous structure. The amount adsorbed rises very steeply at high relative pressure ($P/P0 > 0.8$), which suggests the presence of large mesopores or macropores [26]. The textural porosity should arise from spaces formed by the constituting silica particles in the supports. The BJH method was applied to the desorption isotherm to estimate the pore diameter. The pore size distributions of two samples are both very broad. As shown in the inset of Fig. 3a, there are two peaks centered at 3.5 nm and 18.3 nm in commercial SiO_2. Whereas, in the BJH pore size distribution of SiO_2 hollow spheres (inset of Fig. 3b), there are three peaks around 3.5, 7.6 and 30.5 nm, respectively. This result indicates the structure of SiO_2 hollow spheres is not so homogeneous, which is consistent with the TEM result. Quantitative calculation shows that the BET surface area of commercial SiO_2 and SiO_2 hollow spheres is 526 and 77 m^2/g, respectively.

XRD patterns of hollow spherical catalysts loading different CuO amounts are shown in Fig. 4. The diffraction peaks at 2θ = 32.0°, 35.6°, 38.7° and 48.8° can be attributed to crystalline copper oxide. The peak around 26.2° is ascribed to amorphous SiO_2. For hollow spherical catalyst with CuO loading amount of 2 g/100 g SiO_2, two very weak and wide peaks at 35.6° and 38.7° are observed, indicating the formation of relative small CuO crystalline particles, as shown in curves Fig. 4b. However, for the C-2CuSi catalyst, no peak of the crystalline copper oxide can be observed (Fig. 4a), which indicates that the copper species are highly dispersed in commercial SiO_2. This should be related to different BET surface area of commercial SiO_2 (526 m^2/g) and SiO_2 hollow sphere (77 m^2/g). In addition, as the loading amounts of CuO increasing, the peaks of the

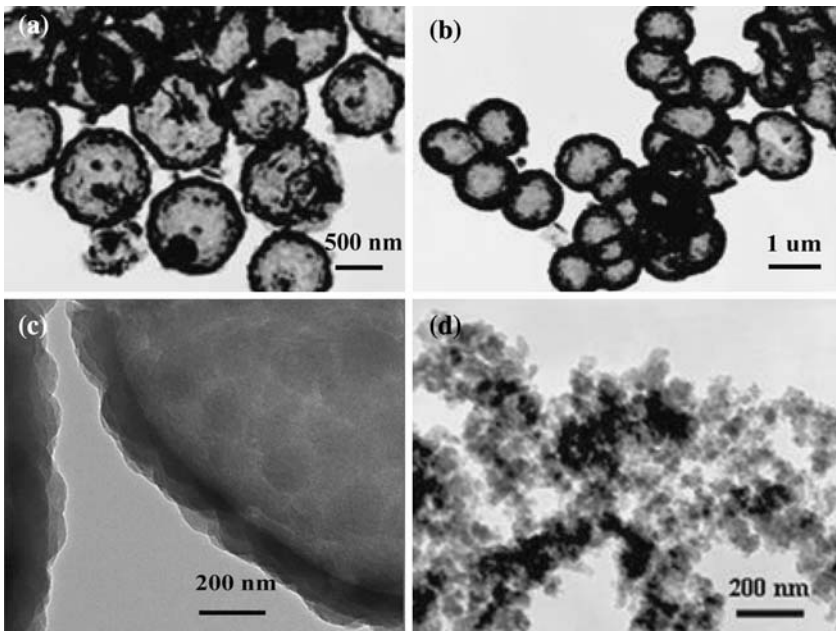

Fig. 2 TEM image of SiO_2 hollow spheres supports (**a**), CuO/SiO_2 hollow spheres catalysts (**b**), locally magnified image of SiO_2 hollow spheres (**c**) and commercial SiO_2 powders (**d**)

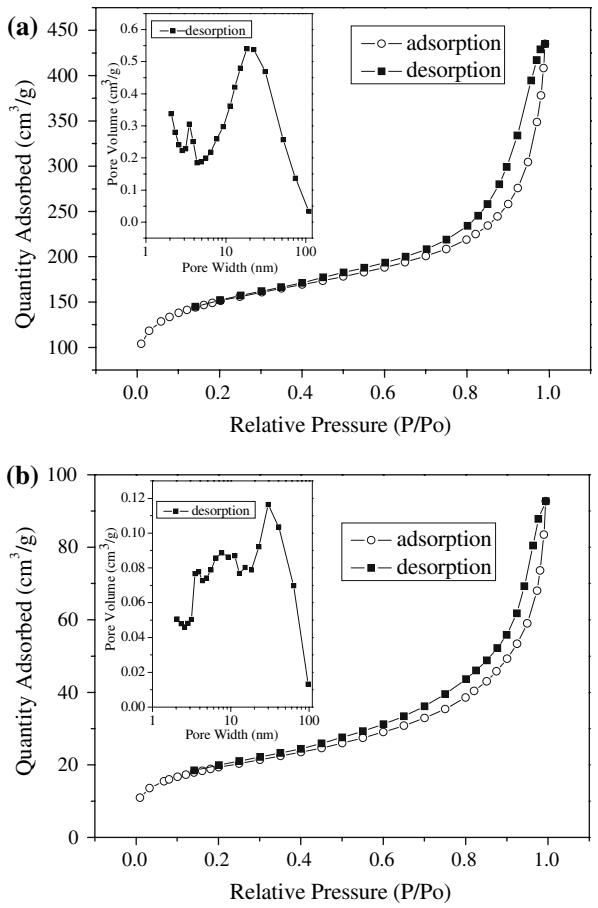

Fig. 3 The nitrogen adsorption–desorption isotherms for commercial SiO_2 (**a**) and SiO_2 hollow spheres (**b**) at 77 K. Inset shows the corresponding BJH pore size distribution curves calculated from desorption branch

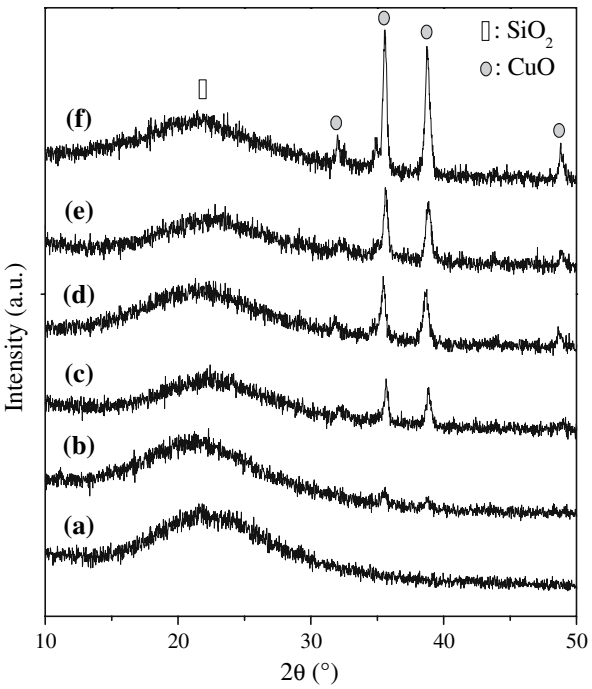

Fig. 4 XRD patterns for CuO/SiO_2 catalysts: (a) C-2CuSi, (b) H-2CuSi, (c) C-10CuSi, (d) H-10CuSi, (e) C-20CuSi and (f) H-20CuSi

crystalline copper oxide become narrower, indicating the formation of larger CuO crystalline particles.

Temperature-programmed reduction, containing some information about the surface structure of the catalysts, has been extensively applied to the characterization of reducible metal oxide catalysts. Figure 5 shows the TPR results of H-xCuSi and C-xCuSi (x = 2, 10, 20) samples with the different copper oxide loading amounts, respectively. For C-xCuSi (x = 2, 10, 20) samples, two reduction peaks centered at about 220 and 300 °C can be observed, as shown in profiles a, c and e, respectively. As reported elsewhere [27, 28], the low temperature reduction peaks should be attributed to the reduction of highly dispersed copper species; while the high temperature reduction peaks should be ascribed to the reduction of bulk CuO. Noticeably, for the samples with the CuO loading amount of 2 g/100 g SiO_2, the reduction peak at 310 °C is very weak, which could be concluded that the main copper species in the C-2CuSi catalyst are highly dispersed. Interestingly, for H-xCuSi (x = 2, 10, 20) catalysts, only one reduction peak centered at about 265 °C can be observed in the TPR profiles b, d and f, respectively. These reduction peaks should be also due to the reduction of crystalline copper oxide particles, and the reduction temperature of CuO crystalline particles in H-xCuSi catalysts is much lower than that in C-xCuSi catalysts. One possibility would be ascribed to the different particle size of crystalline CuO, and the larger crystallites would appear at a higher temperature because of the diffusion hindrance on the reduction process [29]. Another possibility would be related to the unique texture of hollow spheres. Combined with the TEM and BJH pore size distribution results, it should be found that the nanoparticle shells of hollow spheres are porous and this kind of texture should facilitate gas diffusion [30]. In addition, the reduction temperature of CuO crystalline particles in hollow spheres samples shifts to higher temperature with the increasing copper oxide loading amount due to the formation of larger CuO particle. These results are consistent with XRD results.

Figure 6 presents the comparison of CO conversions over H-xCuSi and C-xCuSi catalysts with space velocity of 30,000 mL g^{-1} h^{-1}. The CO conversions over H-xCuSi catalysts are higher than that over C-xCuSi catalysts with the same copper oxide loading amount. These results suggest that, as supports for these catalysts, the SiO_2 hollow sphere is more suitable than commercial SiO_2. In addition, CO conversions of catalysts increase with the reaction temperature, as shown in Fig. 6b and the results

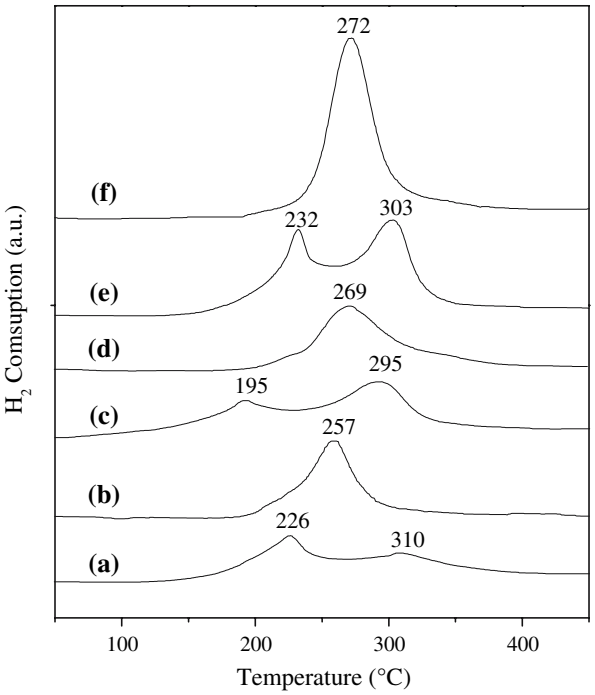

Fig. 5 TPR profiles of CuO/SiO_2 catalysts: (a) C-2CuSi, (b) H-2CuSi, (c) C-10CuSi, (d) H-10CuSi, (e) C-20CuSi and (f) H-20CuSi

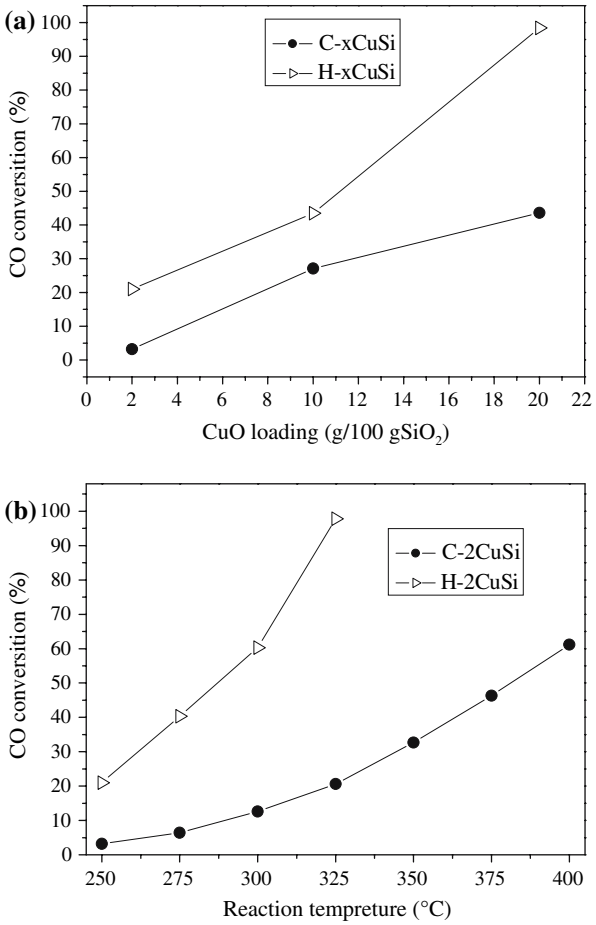

Fig. 6 The catalytic activities of catalysts with different morphology: (**a**) CO conversion of catalysts with different copper oxide loading amounts at 250 °C and (**b**) CO conversion of catalysts with copper oxide loading amounts of 2 g/100 g SiO_2 at different reaction temperature

indicate that the reaction temperature plays an important role in the activity of the CuO/SiO_2 catalysts as well. Although the catalytic results are not superior to some other catalysts, such as supported Au and Pd nanoparticles catalysts [14, 23], the present approach may be of general use in the preparation of catalysts with unique morphology and properties.

To approach clearly the influence of the morphology of SiO_2 supports on the catalytic properties of these catalysts, the turnover numbers of CO molecules were calculated and presented in Table 1. For H-2CuSi sample, the catalyst shows the highest CO turnover number of all samples. Combined with the XRD and TPR results, CuO mainly are small crystalline particles in this sample. However, for copper oxide supported on commercial SiO_2, the turnover number of CO is the lowest. XRD and TPR results reveal that copper species mainly are highly dispersed. Therefore, it could be concluded that the highly dispersed copper species made little contribution to the catalytic activity. For the hollow spherical catalysts with high copper oxide loadings such as 10 and 20 g/100 g SiO_2, the CO turnover numbers decrease to 8.15 and 10.06, respectively. This should be related to the formation of larger CuO particles. Accordingly, it seems to suggest that the main active species in this system should be the small CuO particles, which is consistent with the result proposed by Liu et al. that copper entities active for the CO oxidation involved the small CuO particle [31]. In other words, it should be

Table 1 The turn-over numbers of CO on every copper ions per hour in different catalysts

Catalysts	CuO loading (g/100 g SiO_2)	Turn-over number		
		250 °C	275 °C	300 °C
H-xCuSi	2	18.24	35.01	52.39
	10	8.15	10.44	18.68
	20	10.06		
C-xCuSi	2	2.78	5.56	10.95
	10	5.08	9.15	12.07
	20	4.46	6.21	9.97

concluded that the effect of the copper species on the CO oxidation activity of the CuO/SiO_2 catalysts has the following order: small CuO crystalline particles > larger CuO crystalline particles > highly dispersion copper species. Considering the unique texture of hollow spherical supports, it is suggested that the gaps among SiO_2 particles in

silica hollow spherical supports would restrict the formation of larger CuO particles and numerous small CuO particles would form in these samples. In addition, the influence of unique hollow texture on gas diffusion is another possible factor related to catalytic activity. While the BET surface area of SiO_2 hollow spheres is not so high, it is worth noting that the hollow texture with porosity should facilitate gas diffusion into spheres interior. As a result, both the exterior and the interior of the spheres are accessible to the gases, so the available active surface area of active species CuO is enhanced [30]. However, the CuO crystalline particles in commercial silica sample should be surrounded by silica nanoparticles with the size of about 20 nm, which would retard sufficient contact between reaction gases and active catalytic species. Thus, the CO turnover numbers over these hollow spherical catalysts are higher than those over the C-xCuSi catalysts. Accordingly, it could be considered that the supports with hollow spherical morphology would show unique properties in catalyst preparation, especially for the CO oxidation catalysts.

4 Conclusion

(1) The hollow spheres SiO_2 supports have been prepared by using carbonaceous spheres as templates in a simple sol–gel procedure.

(2) The catalytic activity of CuO supported on hollow spherical SiO_2 exhibited much higher than that supported on commercial SiO_2 for CO + O_2 reaction. The results indicate the effect of the copper species on the CO oxidation activity of the CuO/SiO2 catalysts has the following order: small CuO crystalline particles > larger CuO crystalline particles > highly dispersion copper species. The unique hollow spherical texture of supports should be in favor of the formation of the main active species and gas diffusion in catalysts at current condition.

Acknowledgments The financial supports of the National Natural Science Foundation of China (No. 20573053), and the National Basic Research Program of China (Grant No. 2003CB615804) are gratefully acknowledged.

References

1. Yang Z, Niu Z, Lu Y, Hu Z, Han CC (2003) Angew Chem Int Ed 42:1943
2. Wang D, Luo Q, Jia D, Li X, Wang X, Huang Y, Zhen Z, Liu X (2003) Chin Chem Lett 14:1306
3. Caruso F (2003) Top Curr Chem 227:145
4. Tartaj P, Carreno TG, Serna CJ (2001) Adv Mater 13:1620
5. Wang H, Wang R, Sun X, Yan R, Li Y (2005) Mater Res Bull 40:911
6. Yin J, Qian X, Yin J, Shi M, Zhou G (2003) Mater Lett 57:3859
7. Liang H, Zhang H, Hu J, Guo Y, Wan L, Bai C (2004) Angew Chem Int Ed 43:1540
8. Feng X, Mao C, Yang G, Hou W, Zhu J (2006) Langmuir 22:4384
9. Kim SW, Kim M, Lee WY, Hyeon T (2002) J Am Chem Soc 124:7642
10. Baca M, Li WJ, Du P, Mul G, Moulijn JA, Coppens MO (2006) Catal Lett 109:207
11. Jiang Y, Yang S, Ding X, Guo Y, Bala H, Zhao J, Yu K, Wang Z (2005) J Mater Chem 15:2041
12. Li Y, Zhou P, Dai Z, Hu Z, Sun P, Bao J (2006) New J Chem 30:832
13. Kang M, Song MW, Lee CH (2003) Appl Catal A 251:143
14. Yang Y, Saoud MK, Abdelsayed V, Glaspell G, Deevi S, Shall MSE (2006) Catal Commun 7:281
15. Glaspell G, Abdelsayed V, Saoud KM, Shall MSE (2006) Pure Appl Chem 78:1667
16. Zheng X, Wang S, Wang S, Zhang S, Huang W, Wu S (2004) Catal Commun 5:729
17. Arias AM, Garcia MF, Galvez O, Coronado JM, Anderson JA, Conesa JC, Soria J, Munuera G (2000) J Catal 195:207
18. Yakhnin V, Menzinger M (2006) Chem Eng Sci 61:347
19. Hu Y, Dong L, Shen M, Liu D, Wang J, Ding W, Chen Y (2001) Appl Catal B 31:61
20. Dow WP, Huang TJ (1996) J Catal 160:171
21. Glaspell G, Fuoco L, Shall SME (2005) J Phys Chem B 109:17350
22. Korach L, Czaja K, Bialon JM, Jarzebski A (2006) Eur Polym J 42:3085
23. Glaspell G, Hassan HMA, Elzatahry A, Fuoco L, Radwan NRE, Shall MSE (2006) J Phys Chem B 110:21387
24. Li X, Lou T, Sun X, Li Y (2004) Inorg Chem 43:5442
25. Sun X, Li Y (2004) Angew Chem Int Ed 43:3827
26. Kruk M, Jaroniec M (2001) Chem Mater 13:3169
27. Wang Z, Liu Q, Yu J, Wu T, Wang G (2003) Appl Catal A 239:87
28. Dow W, Wang Y, Huang T (1996) J Catal 160:155
29. Marchi AJ, Fierro JLG, Santamaria J, Monzon A (1996) Appl Catal A 142:375
30. Martinez CJ, Hockey B, Montgomery CB, Semancik S (2005) Langmuir 21:7937
31. Liu W, Sarofim AF, Stephanopoulos MF (1994) Chem Eng Sci 49:4871